Fuel 144 (2015) 171–179

Contents lists available at ScienceDirect

Fuel

journal homepage: www.elsevier.com/locate/fuel

Torrefaction of oil palm kernel shell in the presence of oxygen and carbon dioxide

Yoshimitsu Uemura [a,*], Shazleen Saadon [a], Noridah Osman [a], Nurlidia Mansor [b], Ken-ichiro Tanoue [c]

[a] *Center for Biofuel and Biochemical Research, Universiti Teknologi Petronas, Bandar Seri Iskandar, 31750 Tronoh, Perak, Malaysia*
[b] *Department of Chemical Engineering, Universiti Teknologi Petronas, Bandar Seri Iskandar, 31750 Tronoh, Perak, Malaysia*
[c] *Department of Mechanical Engineering, Yamaguchi University, Tokiwa-dai, Ube, Yamaguchi 755-8611, Japan*

HIGHLIGHTS

- Torrefaction of palm kernel shell was done under N_2, O_2 and CO_2 atmospheres.
- The severity of torrefaction was in the order of $O_2 > CO_2 > N_2$.
- The van Krevelen plots showed the common trend among the three different atmospheres.
- The oxidative torrefaction rate was extracted from the overall torrefaction rate.
- The morphological changes were distinctive among the three different atmospheres.

ARTICLE INFO

Article history:
Received 9 August 2014
Received in revised form 10 December 2014
Accepted 13 December 2014
Available online 27 December 2014

Keywords:
Torrefaction
Palm kernel shell
Oxygen
Carbon dioxide
Solid phase conversion
Morphology

ABSTRACT

Torrefaction of oil palm kernel shell (PKS), one of the biomass residues from the palm oil industry, was carried out in a fixed-bed tubular reactor in the presence of oxygen and carbon dioxide at concentrations ranging from 0 to 15 vol.% (nitrogen balance). The effects of oxygen and carbon dioxide concentrations (0, 3, 9, 12, and 15 vol.%), temperature (493, 523, and 573 K) and biomass size (0.375 mm and unground) on the solid phase conversion, the energy yield and properties of torrefied biomass were investigated. The solid phase conversion increased with increasing temperature and oxygen or carbon dioxide concentration, but was not significantly affected by biomass size. The energy yield decreased with increasing oxygen or carbon dioxide concentration, but was still more than 70%. The extent of torrefaction was in the order of oxygen > carbon dioxide > nitrogen. The 'oxidative torrefaction' rate was extracted from the overall reaction rate. The increase in the oxidative torrefaction rate caused by oxygen was higher than that caused by carbon dioxide. Scanning electron microscope observations of the morphology of the PKS showed distinctive differences for torrefaction in nitrogen, oxygen, and carbon dioxide.

© 2014 Elsevier Ltd. All rights reserved.

1. Introduction

Lignocellulosic biomass is one of the most abundant biomass resources on earth and can be used as a feedstock for preparing fuels and chemicals. Some of these technologies are still under development. Because of its availability in Malaysia, oil palm residues are considered to be the best biomass source [1]. In 2013, Malaysia was the second largest producer of palm oil, producing 19.8 million tons, or 33.4% of the total world supply. Indonesia was the world's largest producer of palm oil, producing 31.0 million tons of oil, or 52.2% of the total world supply [2]. In 2013, productive oil palm plantations in Malaysia covered 5.23 million hectares, a 3.0% increase from 2012 when productive oil palm plantations covered 5.08 million hectares [3]. Types of biomass produced by the oil palm industry include empty fruit bunches (EFB), mesocarp fiber, palm kernel shells (PKS), fronds, and trunks. EFB, mesocarp fiber, and PKS are generated at palm oil mills, whereas fronds and trunks are generated at the plantations [4]. The total amount of this biomass produced annually is 17 Mtoe (million tons of oil equivalent) [1]. Since the current primary energy supply in Malaysia is approximately 70 Mtoe, the total oil palm biomass energy potential of 17 Mtoe may contribute considerably to decreasing the consumption of fossil fuels, such as natural gas, coal, and oil. However, to use biomass waste for energy efficiently, the following drawbacks, compared with the situation for fossil fuels, must be overcome.

---

[*] Corresponding author. Tel.: +60 5 368 7644; fax: +60 5 368 7649.
E-mail address: yoshimitsu_uemura@petronas.com.my (Y. Uemura).

http://dx.doi.org/10.1016/j.fuel.2014.12.050
0016-2361/© 2014 Elsevier Ltd. All rights reserved.

(1) Higher energy consumption during collection
(2) Heterogeneous and uneven composition
(3) Lower calorific value
(4) Higher cost of transportation due to its lower energy density
(5) High ash content
(6) Reduction in quality by biodegradation

A number of options exist to reduce these drawbacks. The most common techniques are pelletization, liquefaction, and gasification of the biomass. Pelletization involves drying, chipping, grinding, and pelletizing lignocellulosic biomass. Pelletization is the cheapest option, but its disadvantages include lower heat values and quality deterioration by moisture (pellet disintegration, moss growth, or bioorganic decomposition). Recently, treatment of biomass at a low temperature of 473–573 K under an inert atmosphere was found to improve the energy density and shelf life of the biomass. This treatment is called 'torrefaction' and has been widely researched for wood and grass biomass over the past few years [5–16]. Torrefaction studies have largely been conducted on wood and grass biomass, including wood dust [10–14,16], beech [6,7], eucalyptus [5,11], willow [6–9,13], larch [6,7], bamboo [13] and canary grass [8].

Although torrefaction is one of the most promising methods for improving lignocellulosic solid fuels, the procedure requires thermal energy and an inert atmosphere. Could flue gas from burners be used, inert gas and a considerable quantity of energy would be saved, making the process more economically viable. In light of this, we have examined the effect of an oxygen atmosphere on the solid and energy yields for EFB torrefaction [17]. Following the first study of oxidative torrefaction, several papers have been published on torrefaction under an oxygen atmosphere [18–22].

Rousset et al. [18] torrefied a large piece (10 × 40 × 80 mm) of eucalyptus under 2–21 vol.% oxygen at 513 and 553 K in a fixed bed reactor, and reported that the solid and energy yields decreased considerably only at 553 K. They did not report results for torrefaction under a nitrogen atmosphere. Lu et al. [19] torrefied oil palm fiber and eucalyptus in nitrogen and air at 523–623 K in a fixed bed reactor, and found that torrefaction in air resulted in lower solid and energy yields than in nitrogen. Wang et al. [20] carried out torrefaction experiments using spruce sawdust in 0–21 vol.% oxygen at 533–573 K using a thermogravimetric analyzer and a fluidized bed, and concluded that the presence of oxygen results in slightly poorer torrefaction. Chen et al. [21] torrefied five types of biomass, oil palm fiber (<30 mm), coconut fiber (<30 mm), eucalyptus (15 × 10 × 5 mm) and *Cryptomeria japonica* (15 × 10 × 5 mm), in 0–21 vol.% oxygen at 573 K in a fixed bed reactor and drew a similar conclusion to Wang et al. [20]; that is, non-oxidative torrefaction produces better results than oxidative torrefaction. Chen et al. also investigated the effect of the superficial velocity of the torrefaction gas on the performance of oxidative torrefaction [22].

All of the findings of the above-mentioned studies were reported in relatively quick succession. However, knowledge of torrefaction of agricultural residues under an oxygen atmosphere is still insufficient. There has also been no comprehensive study of torrefaction under oxygen and carbon dioxide, which are the two major components in flue gases. Therefore, oxidative torrefaction must be studied further to find out whether burner flue gases can be used for torrefaction of biomass from the palm oil industry. Investigating how carbon dioxide affects the torrefaction process is of particular importance. Only one paper has been published on torrefaction under carbon dioxide to date and only pure carbon dioxide was used [23], whereas concentrations of carbon dioxide in burner flue gases typically range from 6 to 14 vol.% [24].

In this paper, torrefaction of PKS was carried out in a fixed-bed tubular reactor in the presence of oxygen and carbon dioxide from 0 to 15 vol.%. The effects of oxygen and carbon dioxide concentrations, temperature, and biomass size on the solid phase conversion, energy yield, and properties of torrefied biomass were investigated.

2. Experimental

2.1. Biomass samples

PKS was collected from an oil palm plantation at Bota in Perak, Malaysia. After drying at 378 K for 24 h, the PKS was ground using a mechanical grinder. The ground powders were sieved into 0.25–0.50 mm powder, which has a nominal average diameter of 0.375 mm. The dried unground and ground sieved particles were used in the present study. The fundamental properties of the PKS are summarized in Table 1.

The ground and sieved particles (0.375 mm in average diameter) were used to examine torrefaction in a biomass size range free from heat and mass transfer effects. By comparing the results from unground and 0.375 mm particles, the extent of the heat and mass transfer effects can be determined.

2.2. Torrefaction experiment

Torrefaction of the PKS biomass samples was carried out at an ambient pressure using a vertical tubular reactor made of stainless steel, with an internal diameter of 0.028 m. Approximately 3 g of PKS was placed in the reactor. After flushing the reactor with torrefaction gas for 15 min, the temperature of the reactor was increased to the desired level (493, 523, or 573 K), at a constant rate of 10°/min, using an electric furnace surrounding the reactor. The temperature range of 493–573 K was chosen because the selective decomposition of hemicelluloses occurs between 473 and 573 K. The minimum temperature of 493 K was selected because the torrefaction rate below 493 K would be too low. After torrefaction for 30 min, the heater was turned off and the reactor was left to cool to ambient temperature. The torrefied sample was then recovered, weighed, and stored in an airtight vessel until it was characterized. Throughout the procedure, 30 mL/min of torrefaction gas was passed through the reactor. The concentration of oxygen or carbon dioxide in the gas was adjusted to 0, 3, 9, 12, or 15 vol.%, to investigate the effect of oxygen or carbon dioxide concentration on torrefaction. The concentration ranges of oxygen and carbon dioxide were chosen because flue gases from burners and boilers contain 6–14 vol.% oxygen and 1–13 vol.% carbon dioxide [24]. The torrefaction gas was prepared by mixing nitrogen and compressed air or carbon dioxide under ambient pressure.

Table 1
Proximate, elemental, calorific and fiber analyses of palm kernel shell used in this study.

Proximate analysis (wt.%)	
Moisture	10.0
Volatile matter	70.5
Fixed carbon	18.7
Ash	0.84
Elemental analysis (wt.%)	
C	50.62
H	6.02
N	0.37
O	42.15
HHV [MJ/kg]	20.1
Chemical composition analysis (wt.%)	
Hemicellulose	18.2
Cellulose	33.2
Lignin	48.6

The contribution of torrefaction reaction during temperature rise (20, 23 and 28 min for 493, 523 and 573 K torrefaction, respectively) to the torrefaction reaction during the constant temperature (30 min) was estimated from the linear temperature rise pattern (10°/min) using a representative activation energy of torrefaction, 145.9 kJ/mol [20]. The reaction during the temperature rise to that during the constant temperature was estimated to be 6.2, 6.8 and 7.7% for 493, 523 and 573 K torrefaction, respectively. The contribution during cooling down is expected to be less than that of temperature rise discussed above since the temperature pattern of cooling down is steeper than the linear pattern of temperature rise.

2.3. Measurements

Two samples of different diameters were used in this study. Their masses and the calorific values were measured before and after torrefaction. Calorific values were measured using a bomb calorimeter (C2000, IKA Werke). The calorific value obtained from the bomb calorimeter was the high heat value (HHV), which included the latent heat of the vapor emitted from the specimen. Using the results of the torrefaction experiments, two variables, the solid phase conversion X_S and the energy yield y_E, were calculated using the following two equations:

$$X_S = \frac{M_0 - M_t}{M_0} \tag{1}$$

$$y_E = \frac{M_t}{M_0}\frac{\mathrm{HHV}_t}{\mathrm{HHV}_0} \tag{2}$$

where M is the mass of sample in kg, the subscript 0 means the initial value before torrefaction, the subscript t means the value after torrefaction.

The elementary analysis of untorrefied and torrefied biomass samples was carried out by using a CHN analyzer (Series II CHNS/O Analyzer 2400, Perkin Elmer). Morphological differences in cross sections of untorrefied and torrefied biomass samples were observed by scanning electron microscopy (SEM; Hitachi, TM3030). The cross section of each sample was coated with a thin layer of gold using a gold coater before SEM measurements.

3. Results and discussion

3.1. Solid phase conversion

3.1.1. Torrefaction in nitrogen

3.1.1.1. Effect of torrefaction temperature on solid phase conversion. Fig. 1(a) and (b) shows the solid phase conversion as a function of torrefaction temperature for the 0.375 mm and unground PKS particles, respectively. At more than 50% of the experimental conditions, the experiment was repeated twice for checking reproducibility. The standard deviation of the solid phase conversion ranged from 0.18 to 1.87, 0.01 to 1.56 and 0.44 to 1.24 for nitrogen, oxygen and carbon dioxide, respectively. The atmosphere was changed from inert (pure nitrogen) to 15 vol.% oxygen (nitrogen balance). The atmospheres were pure nitrogen, and 3, 9, 12 and 15 vol.% oxygen in nitrogen. The solid phase conversion in an inert atmosphere increased monotonically with the increase in torrefaction temperature. The increase for both the 0.375 mm and unground PKS show saturation behavior, in which the slope decreases gradually with temperature. This saturation may be attributed to the fact that the major reactant in torrefaction is hemicellulose [25], which runs out at the highest temperature of 573 K under the present conditions. Since the hemicellulose content in PKS is 18.2 wt.% (Table 1), the increase in the solid phase conversion will be hindered above 18.2%. The maximum conversion observed in Fig. 1 for inert torrefaction is however 32%, which is higher than 18.2%. This discrepancy may be attributed to partial decomposition of cellulose. Chen and Kuo [26] reported that cellulose also decomposes by 50% at 563 K under nitrogen atmosphere, whereas very little decomposition was observed at 533 K. In this study, the hemicellulose content of torrefied PKS was not measured since already many papers [8,13,26] proved that the major reactant of torrefaction is hemicellulose. Bridgeman et al. [8] reported torrefaction of three types of biomass, and found that willow containing the least amount of hemicellulose among the three showed the lowest mass loss. Chen and Kuo [13] studied torrefaction of four types of biomass using the TGA technique, and found hemicellulose is consumed preferentially by torrefaction. Chen and Kuo [26] studied torrefaction of hemicellulose, cellulose and lignin, and found that hemicellulose is the component which decomposes most at the torrefaction temperature range.

(a) 0.375 mm particle

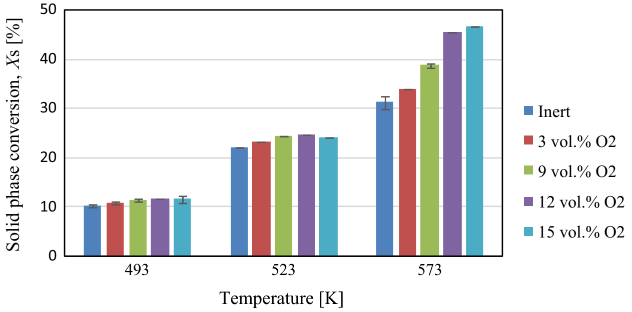

(b) unground particle

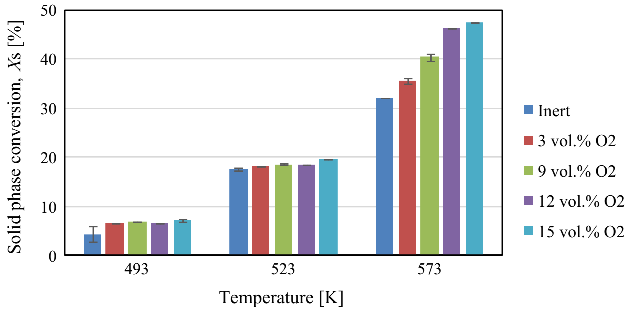

Fig. 1. Solid phase conversion of (a) 0.375 mm and (b) unground particles under oxygen atmospheres as a function of temperature.

3.1.1.2. Effect of biomass particle size on solid phase conversion. In an inert atmosphere, the solid phase conversion of 0.375 mm (Fig. 1(a)) is larger than that of unground PKS (Fig. 1(b)) at the lower two temperatures of 493 and 523 K. At 493 K, the solid phase conversion of 0.375 mm (10.2%) is larger than that of unground (4.3%). Similarly, at 523 K, the solid phase conversion of 0.375 mm (22.1%) is larger than that of unground (17.7%). This difference arises from the heat transfer control for unground particles. In contrast, at the highest temperature of 573 K, the solid conversion of the unground sample (32.1%) shows no significant difference to that of 0.375 mm (31.3%). Pyle and Zaror [27] proposed a scheme for predicting the relative significance of the three representative rates for biomass decomposition, including the intrinsic reaction rate, external heat transfer, and internal heat transfer. They proposed the three parameters including the Biot number, *Bi*, the Pyrolysis number, *Py*, and the Second Pyrolysis number, Py'. The parameters are defined by the following three equations:

$$Bi = \frac{\tau(internal\ heat\ transfer)}{\tau(external\ heat\ transfer)} = \frac{\alpha\, r_P}{\lambda} \tag{3}$$

$$Py = \frac{\tau(reaction)}{\tau(internal\ heat\ transfer)} = \frac{\lambda}{k\ \rho\ C_P\ r_P^2} \tag{4}$$

$$Py' = Py\ Bi = \frac{\tau(reaction)}{\tau(external\ heat\ transfer)} = \frac{\alpha}{k\ \rho\ C_P\ r_P} \tag{5}$$

where α is the external heat transfer coefficient in W/(m^2 K), k is the reaction rate constant in s^{-1}, ρ is the density in kg/m^3, C_P is the heat capacity in J/(kg K), r_P is the radius in m, and λ is the thermal conductivity in W/(m K) of the biomass particles.

The values of *Py* are the criterion if either the intrinsic reaction or the internal heat transfer is the controlling factor. The higher the value, the more the intrinsic reaction is the controlling factor. Since the value of *Py*(0.375 mm)/*Py*(unground) is constant (711) throughout the three different temperatures, Pyle and Zaror's scheme cannot explain the following trend in Fig. 1(a) and (b):

> At 493 and 523 K: X_s(0.375 mm) > X_s(unground); consistent with Pyle and Zaror's scheme
> At only 573 K: X_s(0.375 mm) ≈ X_s(unground); inconsistent with Pyle and Zaror's scheme

Thus, the cause of this trend, in which the solid phase conversion between two distinctive sizes of PKS shows a similar value at the highest torrefaction temperature of 573 K, must be explained. The pyrolysis behavior of the major components in lignocellulose reported by Yang et al. may account for the trend [28]. They reported that pyrolysis of hemicellulose showed an exothermic peak at 550 K and lignin at 640 K. This exothermic effect at 550–640 K may be attributed to the anomalistic trend at 573 K, which is not explained by Pyle and Zaror's scheme.

3.1.2. Torrefaction in oxygen

In this section, the effects of the torrefaction temperature and oxygen concentration on the solid phase conversion will be discussed. From Fig. 1(a) and (b), there are two obvious trends.

(1) Oxygen affects the solid phase conversion only at the highest temperature of 573 K.
(2) The effect of oxygen at 573 K is greater at higher oxygen concentrations.

In general, this increase in solid phase conversion by oxygen is recognized as the partial combustion of biomass. To examine the effect of oxygen, $X_s(O_2)$–$X_s(N_2)$ (solid phase conversion enhanced by oxygen) is plotted against the torrefaction temperature in Fig. 2(a) and (b). The first of the two obvious trends above can be explained by the partial combustion becoming significant above a threshold temperature. Rousset et al. reported that the torrefaction rate at 553 K was enhanced by oxygen, whereas it was not enhanced by oxygen at 513 K (2, 6, 10, and 21 vol.%) [18]. In Fig. 2(a) and (b), the value of $X_s(O_2)$–$X_s(N_2)$ is monotonically increased by the increase in oxygen concentration. A similar increase was observed for the oxidative torrefaction of palm oil EFB in our previous study [17] and by Rousset et al. [18]. The increase reaches saturation at 12–15 vol.% oxygen in this study; this was not reported in previous papers, in which the effect of oxygen concentration on torrefaction was investigated [18,21]. This discrepancy may be attributed to the different biomass used; PKS is used in the present study, whereas wood and fiber biomass was used in the previous two papers [18,21]. Biomass particle size did not have a significant effect on $X_s(O_2)$–$X_s(N_2)$ (Fig. 2(a) and (b)).

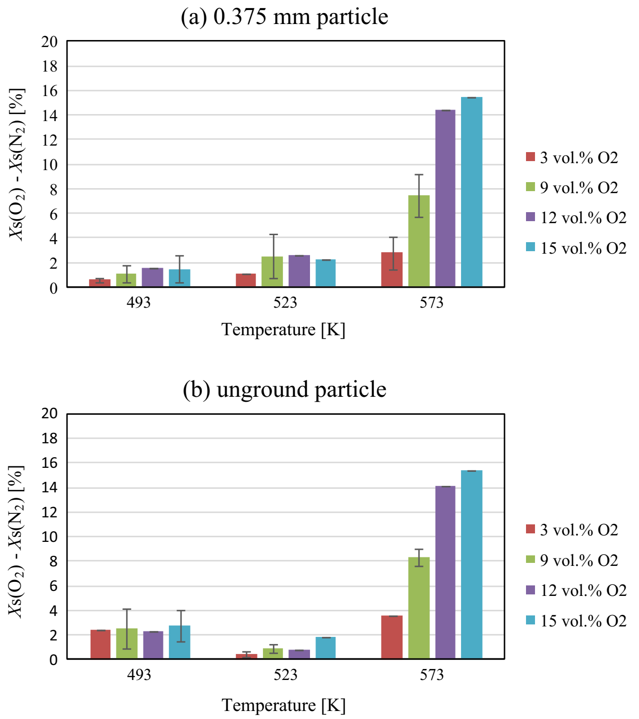

Fig. 2. Solid phase conversion of (a) 0.375 mm and (b) unground particles enhanced by oxygen as a function of temperature.

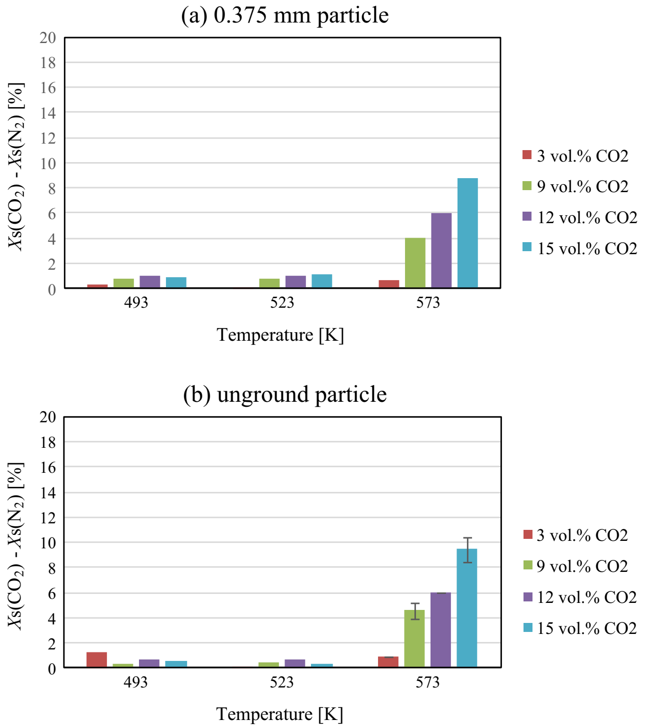

Fig. 3. Solid phase conversion of (a) 0.375 mm and (b) unground particles enhanced by carbon dioxide as a function of temperature.

3.1.3. Torrefaction in carbon dioixde

Fig. 3(a) and (b) shows $X_s(CO_2)$–$X_s(N_2)$ (solid phase conversion enhanced by carbon dioxide) as a function of torrefaction temperature for 0.375 mm and unground PKS, respectively. The general trend is similar to that in oxygen shown in Fig. 2(a) and (b).

(1) Carbon dioxide affects the solid phase conversion only at the highest temperature of 573 K.
(2) The effect of carbon dioxide at 573 K is more significant at higher carbon dioxide concentrations.

Therefore, we examined how carbon dioxide enhanced torrefaction. There is only one previous report of torrefaction in carbon dioxide [23], in which torrefaction of woody biomass at 473–573 K in pure carbon dioxide was compared with ordinary torrefaction in pure nitrogen. The authors did not observe the enhancing effect of carbon dioxide at lower temperatures of 473–493 K, whereas a 10–20% enhancement was observed at 533–573 K. However, no specific mechanism for the effect of carbon dioxide was proposed.

There may be a physical and a chemical effect that could explain the enhancing effect. The possible physical effect may arise if the thermal conductivity of carbon dioxide is higher than that of nitrogen. If this is the case, carbon dioxide may allow a higher heat transfer via the surface gas film. However, the thermal conductivity of carbon dioxide is 32 mW/(m K), and is smaller than that of nitrogen, 43 mW/(m K) at 573 K. Consequently, this physical effect is unlikely. The chemical effect may occur through the Boudard reaction, in which carbon dioxide reacts with carbon to form carbon monoxide. Activated carbon made from PKS (K.D. Technology Sdn. Bhd., Kuala Lumpur, Malaysia) was torrefied at 573 K under 15 vol.% carbon dioxide in the present study, to determine whether the Boudart reaction occurs under the conditions. This experimental run showed a solid yield of 77.3% and a CO yield of 0.11%. These results show the enhancing effect of carbon dioxide can be attributed to the Boudart reaction.

The main difference between oxygen and carbon dioxide is that $X_s(O_2)$–$X_s(N_2)$ of oxygen torrefaction (Fig. 2(a) and (b)) is 1.5–2 times higher than $X_s(CO_2)$–$X_s(N_2)$ of carbon dioxide torrefaction (Fig. 3(a) and (b)). This difference implies that the Boudart reaction is not as fast as partial combustion at 573 K.

3.1.4. Reaction kinetics of PKS torrefaction in the presence of oxygen and carbon dioxide

As discussed in our previous paper [17], the overall torrefaction reaction appears to proceed in two ways. The first is through the decomposition of hemicellulose in ordinary torrefaction, and the other is through partial oxidation or the Boudard reaction of the entire biomass, as follows:

$$\begin{aligned} -r_{\mathrm{overall}} &= (-r_{\mathrm{torref}}) + (-r_{\mathrm{oxy}}) \\ &= k_{\mathrm{torref}}C_{\mathrm{HC}} + k_{\mathrm{oxy}}C^{l}_{\mathrm{PKS}}C^{m}_{\mathrm{O_2}} \qquad \text{(in oxygen)} \end{aligned} \tag{6}$$

$$\begin{aligned} -r_{\mathrm{overall}} &= (-r_{\mathrm{torref}}) + (-r_{\mathrm{Boudard}}) \\ &= k_{\mathrm{torref}}C_{\mathrm{HC}} + k_{\mathrm{Boudard}}C^{l}_{\mathrm{PKS}}C^{n}_{\mathrm{CO_2}} \qquad \text{(in carbon dioxide)} \end{aligned} \tag{7}$$

where $-r$ is the reaction rate of PKS in kg/(m^3 s), k_{torref} is the rate constant of torrefaction in s^{-1}, k_{oxy} is the rate constant of oxidation in kg^{1-l} m$^{3(l+m-1)}$ mol^{-m} s^{-1}, k_{Boudard} is the rate constant of the Boudard reaction in kg^{1-l} m$^{3(l+n-1)}$ mol^{-n} s^{-1}, C_{HC} is the concentration of hemicellulose in PKS in kg/m^3, C_{PKS} is the concentration of PKS in kg/m^3, $C_{\mathrm{O_2}}$ is the concentration of oxygen in mol/m^3, and $C_{\mathrm{CO_2}}$ is the concentration of carbon dioxide in mol/m^3.

Next, the enhancement of the overall torrefaction by oxygen or carbon dioxide is discussed. The enhanced part of the torrefaction reaction rate is expressed by the second term of Eqs. (6) and (7) as:

$$-r_{\mathrm{oxy}} = -\frac{dC_{\mathrm{PKS}}}{dt} = k_{\mathrm{oxy}}C^{l}_{\mathrm{PKS}}C^{m}_{\mathrm{O_2}} \tag{8}$$

$$-r_{\mathrm{Boudart}} = -\frac{dC_{\mathrm{PKS}}}{dt} = k_{\mathrm{Boudart}}C^{l}_{\mathrm{PKS}}C^{n}_{\mathrm{CO_2}} \tag{9}$$

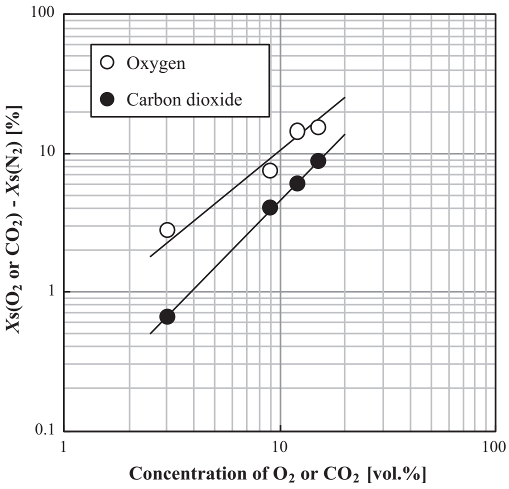

Fig. 4. Reaction order for oxygen and carbon dioxide concentrations.

(a) 0.375 mm particle/O_2

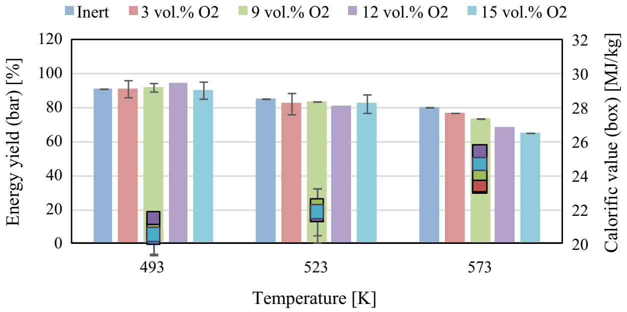

(b) unground particle/O_2

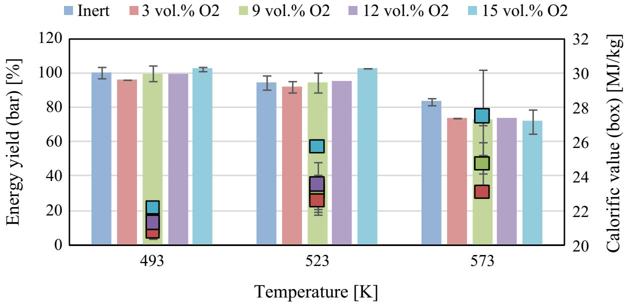

Fig. 5. Energy yield for torrefaction of (a) 0.375 mm and (b) unground particles under oxygen atmospheres as a function of temperature.

Since the enhanced part of the torrefaction conversion is less than 15% in this study, Eqs. (8) and (9) can be simplified to:

$$\frac{-r_{\mathrm{oxy}}}{C_{\mathrm{PKS,\,0}}} = \frac{dx_{\mathrm{PKS}}}{dt} = k^{*}_{\mathrm{oxy}}C^{m}_{\mathrm{O_2}} \tag{10}$$

$$\frac{-r_{\mathrm{Boudart}}}{C_{\mathrm{PKS,\,0}}} = \frac{dx_{\mathrm{PKS}}}{dt} = k^{*}_{\mathrm{Boudart}}C^{n}_{\mathrm{CO_2}} \tag{11}$$

As the concentrations of oxygen and carbon dioxide do not produce a significant change throughout the reactor and during the reaction time, the integrated forms are:

$$x_{\mathrm{PKS}} = k^{*}_{\mathrm{oxy}}C^{m}_{\mathrm{O_2}}t \tag{12}$$

$$x_{\mathrm{PKS}} = k^{*}_{\mathrm{Boudart}}C^{n}_{\mathrm{CO_2}}t \tag{13}$$

(a) 0.375 mm particle/CO_2

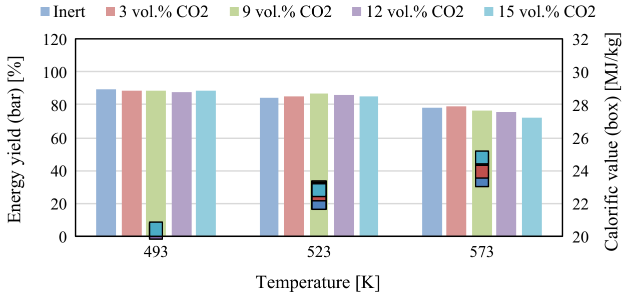

(b) unground particle/CO_2

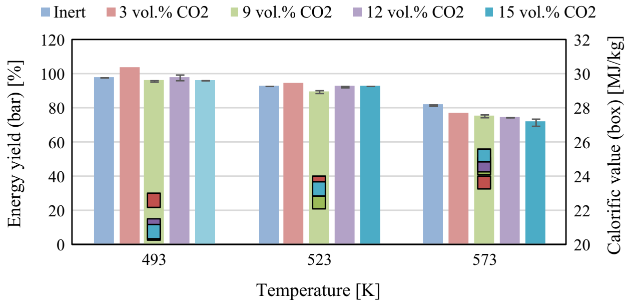

Fig. 6. Energy yield for torrefaction of (a) 0.375 mm and (b) unground particles under carbon dioxide atmospheres as a function of temperature.

Fig. 4 shows plots of $Xs(O_2)–Xs(N_2)$ vs. C_{O_2} and $Xs(CO_2)–Xs(N_2)$ vs. C_{CO_2}, and the parameters m and n in Eqs. (12) and (13) were determined to be 1.2 and 1.7, respectively.

The reaction order of the enhanced part of the torrefaction by oxygen is estimated to be 1.2. Henrich et al. [29] reported the reaction orders for the combustion of municipal waste char, electric scrap char, graphite, and soot as 0.60, 0.50, 0.39, and 0.81, respectively. Senneca [30] reported 0.9, 0.9, and 1.0 for wood chip char, olive husk char, and pine seed shells, respectively. The reaction order of the present study (1.2) is close to those of the previous studies.

The reaction order of the enhanced part of the torrefaction by carbon dioxide is estimated to be 1.7. In the only previous paper examining CO_2 torrefaction [23], the empirical investigation was only carried out in pure carbon dioxide. Therefore, we extended the literature survey scope to gasification of char by carbon dioxide. Recent representative papers reported 0.1–0.5 [31] and 0.9–1.0 [32] as the order of this reaction, which are not consistent with the order obtained in this study. This higher order might be affected by the adsorption of carbon dioxide on carbonaceous material. If it is the case, the higher order of 1.7 in the present study may be explained by Freundlich adsorption, in which the order ranges from 1.4 to 3.1 for the CO_2/char system [33].

3.2. Energy yield

The energy yield for torrefaction in oxygen and carbon dioxide are shown in Figs. 5 and 6 together with the calorific value. Some experimental runs were repeated twice for checking reproducibility. The standard deviation of the energy yield ranged from 1.25 to 2.81 and 0.08 to 4.36 for nitrogen and oxygen, respectively. In Fig. 5(b), the energy yield is slightly higher than 100% at two conditions. It is unlikely that the energy yield exceeds 100% for torrefaction experiment. This may be attributed to the facts:

(1) There is higher uncertainty for torrefaction in oxygen (maximum standard deviation 4.36) than that in nitrogen (maximum standard deviation 2.81).
(2) The energy yield value is found to be very close to 100% for larger biomass size, when Fig. 5(b) is compared with Fig. 5(a). Higher energy yields than 100% are found in one of the previous papers for torrefaction in oxygen at 513 and 553 K, in which a large biomass was used [18]. This trend is more prominent for the lower torrefaction temperature 513 K, and is consistent with the results observed in the present study (Fig. 5(b)).

Except for the anomaly described above, the following three trends are observed in Figs. 5 and 6.

Table 2
Energy yields of fibers, softwoods, and hardwoods.

Group code	Temp. (K)	O_2 conc. (vol.%)	Energy yield (%)				Origin and remarks
A						PKS	Present study
	573	3				75	
	573	15				64	
B						Eucalyptus Hardwood	Ref. [18]10 × 40 × 80 mm in size
	553	6				99	
	553	10				100	
	553	21				98	
C			Oil palm fiber Fiber			Eucalyptus Hardwood	Ref. [19]
	573	21	33.6			54.4	
D					Saw dusts (spruce) Softwood		Ref. [20]
	563	3			74		
E			Oil palm fiber Fiber	Coconut fiber Fiber	*Cryptomeria japonica* Softwood	Eucalyptus Hardwood	Ref. [21]
	573	5	57	52	57	72	
	573	15	40	33	46	64	

PKS: palm kernel shell.

(1) At the lower two temperatures of 493 and 523 K, the presence of oxygen or carbon dioxide had a small effect on the energy yield, regardless of the PKS particle size.
(2) At the highest temperature of 573 K, the oxygen or carbon dioxide concentration had a significant effect on the energy yield.
(3) The energy yields of unground particles at 493 and 523 K were good (90–100%) compared with the other conditions.

Trends (1) and (2) are consistent with the small effect of oxygen or carbon dioxide on the solid phase conversion at the lower two temperatures (Figs. 2 and 3) and the small effect of oxygen or carbon dioxide on the calorific value at the lower two temperatures (Figs. 5 and 6). Chen et al. [22] reported a similar trend for eucalyptus torrefaction in nitrogen and air at 523 and 573 K.

Trend (3) may arise from the higher mass yield for unground particles compared with 0.375 mm particles (Fig. 1). This higher mass yield may be attributed to the heat transfer limitation in larger biomass particles [27], and secondary tar cracking into char inside the biomass during torrefaction. Rousset et al. [18] reported high energy yields (98–100%) for torrefaction of pieces of eucalyptus of 10 × 40 × 80 mm in size in oxygen (6–21 vol.%) at 553 K.

Previous results for torrefaction in oxygen are compared with the present results in Table 2. The data at higher temperatures were chosen to see more clearly the effects of oxygen concentration and biomass type. Higher oxygen concentrations in torrefaction gas resulted in lower energy yields (Groups A and E in Table 2). This can be attributed to greater partial oxidation. Table 2 shows that the order of the energy yield is hardwood > softwood > fiber. This trend may be attributed to the fact that the particle density of hardwoods (0.4–0.7 g/cm^3) is greater than that of softwoods (0.3–0.5 g/cm^3) [34]. The denser the material, the lower the mass loss, which may produce a higher energy yield. PKS (Group A in Table 2) showed similar energy yields to eucalyptus (Group E in Table 2). This may be because of PKS's high particle density (1.25 g/cm^3, measured by the glass bead replacement method).

3.3. Elementary composition of torrefied biomass

Fig. 7(a–d) shows the van Krevelen plot for the four groups of samples: 0.375 mm/O_2, unground/O_2, 0.375 mm/CO_2 and unground/CO_2, respectively. In general, the torrefied samples are located from right top to left bottom in order of increasingly extreme conditions in this plot. The general trends are consistent with those of previous papers under nitrogen [8,21,35] and oxygen [21] atmospheres. The dotted line in each figure shows the trend under an inert atmosphere. The solid line shows the trend under an oxygen or a carbon dioxide atmosphere. Ideally, the effect of oxygen or carbon dioxide should be discussed at each concentration. But the data fluctuation inhibited such an attempt. In this study, we therefore focus on comparison of nitrogen atmosphere with oxygen or carbon dioxide atmosphere. The dotted line (inert) is less steep than the solid line (oxygen or carbon dioxide) regardless of the PKS particle size and torrefaction gas (oxygen and carbon dioxide). However still this difference between inert and oxygen or carbon dioxide is not clear enough in comparison with the fluctuation of the data shown in Fig. 7. Thus further investigation is required to clarify this matter.

3.4. Morphological changes

Fig. 8 shows SEM photographs of untorrefied PKS, and PKS torrefied under nitrogen, oxygen, and carbon dioxide at 493 and 573 K. The untorrefied PKS sample shows layers of football-shaped structures stacked together in parallel along the long axis. Each layer has many small round bumps protruding, which appear as small dimples when observed from the inside. For the lower torrefaction temperature (493 K) in Fig. 8(b–d), a partially melted structure for all the torrefied samples is observed, regardless of the atmosphere. This change may be caused by the softening of lignocellulose, because the glass transition temperatures of hemicellulose, cellulose, and lignin are below or around the torrefaction temperature of 493 K. Lewin and Goldstein [36] reported that the glass transition temperatures of hemicellulose, cellulose, and lignin are 453, 503, and 473 K, respectively. Recently, the glass transition temperatures of Acetosolv lignin and Milox lignin have been reported as 423 and 417 K, respectively [37]. At this lower temperature, the

(a) 0.375mm particle/O_2

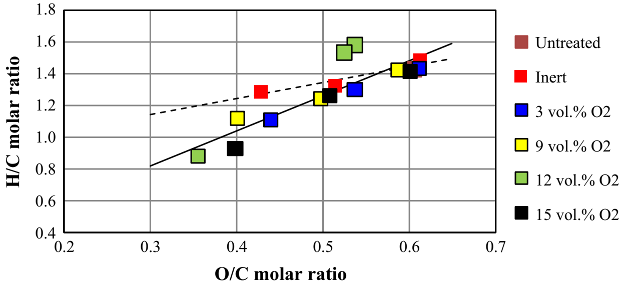

(b) unground particle/O_2

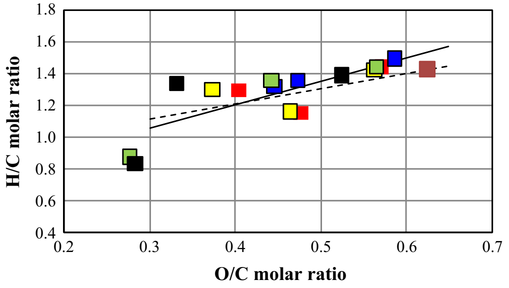

(c) 0.375mm particle/CO_2

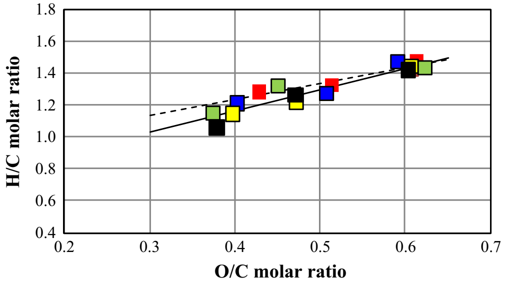

(d) unground particle/CO_2

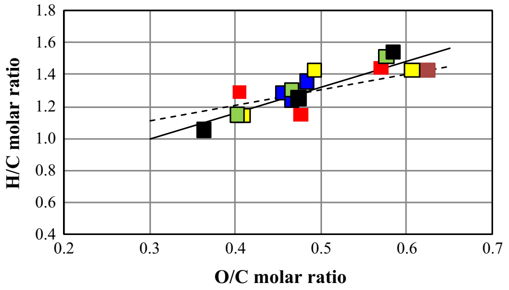

Fig. 7. van Krevelen diagram for torrefaction of (a) 0.375 mm and (b) unground particles under oxygen atmospheres, (c) 0.375 mm and (d) unground particles under carbon dioxide atmospheres.

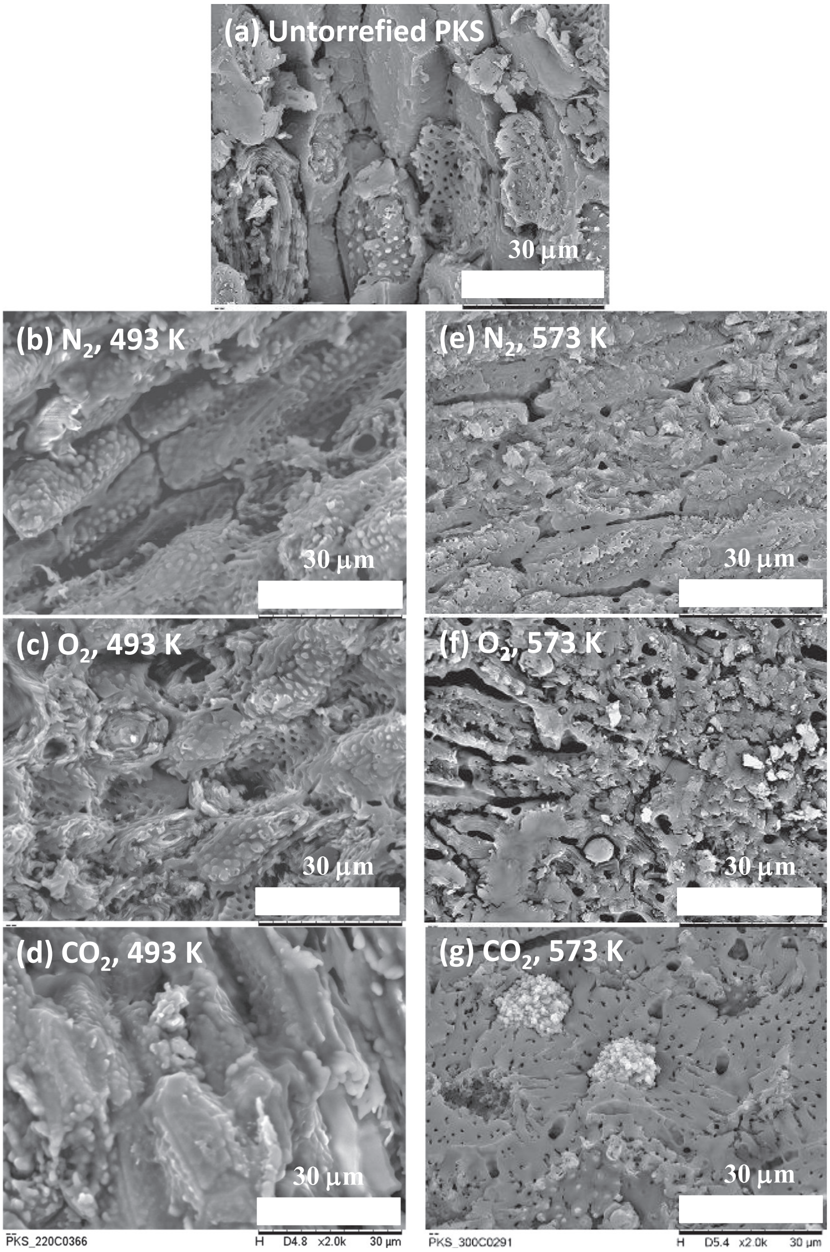

Fig. 8. Cross-sectional morphology (a) before and after torrefaction at 493 K in (b) nitrogen, (c) oxygen, and (d) carbon dioxide; after torrefaction at 573 K in (e) nitrogen, (f) oxygen, and (g) carbon dioxide.

solid phase damage by thermal decomposition was too small to be observed. The insignificant decomposition at 493 K is consistent with the results shown in Fig. 1. Therefore, it is likely that the partially melted structure (Fig. 8(b–d)) is a result of softening rather than decomposition of lignocellulose. When the torrefaction temperature was increased from 493 to 573 K, the softened structure at 493 K disappeared. Instead, three different structures appeared, depending on the atmosphere. Under a nitrogen atmosphere, the layered-football structure shrank and broke, although the football shape remained (Fig. 8(e)). Under an oxygen atmosphere, the breakdown was more complete than under nitrogen (Fig. 8(f)): the football shape almost completely disappeared. Under a carbon dioxide atmosphere, the layered structure decomposed in a different way. Each of the football structures was ripped apart and the layered structure was flattened (Fig. 8(g)). Unexpectedly, the surface of the flattened layers was smooth. It is unsurprising that the three different atmospheres resulted in three different morphological changes at 573 K, because the major reactions are different, as discussed in Sections 3.1.1–3.1.3.

Almeida et al. [11] observed transversal sections of woody biomass torrefied in nitrogen at 453–553 K by SEM, and reported that crack formation was observed at the highest temperature, 553 K. The morphological change under nitrogen at 573 K observed in the present study (Fig. 8(e)) may be caused by a similar mechanism. Chen et al. [21] reported SEM observations of oil palm fiber, coconut fiber, eucalyptus, and *Cryptomeria japonica* torrefied in oxygen (5–21 vol.%) at 573 K for 1 h. The structure of the torrefied biomass in oxygen was more damaged compared with that torrefied in nitrogen. This is consistent with the results shown in Fig. 8(e) and (f). There are no previous reports of morphological changes caused by torrefaction in carbon dioxide.

4. Conclusions

Torrefaction of oil PKS was carried out in the presence of oxygen and carbon dioxide to investigate the effects of the atmosphere on the torrefaction. Both oxygen and carbon dioxide increased the solid phase conversion; particularly at the highest torrefaction temperature of 573 K. Oxygen increased the conversion more than carbon dioxide. The calorific value was also enhanced by both oxygen and carbon dioxide, particularly at 573 K. The energy yield was decreased by the presence of oxygen and carbon dioxide, especially at 573 K.

SEM observations showed that the morphological changes in the biomass caused by torrefaction were distinct for nitrogen, oxygen, and carbon dioxide atmospheres at 573 K. The distinctive changes reflect the different solid decomposition mechanisms as follows:

(1) In pure nitrogen, the hemicellulose methoxyl groups decompose thermally.
(2) In oxygen (nitrogen balance), partial combustion contributes to the overall reaction.
(3) In carbon dioxide (nitrogen balance), the Boudard reaction contributes to the overall reaction.

Furthermore, torrefaction in the presence of oxygen and carbon dioxide can be carried out without any significant problems at 493 and 523 K. Additional mass and energy losses only occur at the highest temperature of 573 K.

Acknowledgments

This work was financially supported by the Mitsubishi Corporation Education Trust Fund. The authors thank Mr. Mohamed Nour-Dine and Mr. Mohammad Hisham Sulaiman of the Center for Biofuel and Biochemical Research for assistance with SEM measurement and manuscript preparation, respectively.

References

[1] Rajab AH. Oil palm biomass residue in Malaysia: availability and sustainability. Int J Biomass Renew 2013;2(1):13–8.
[2] Foreign Agricultural Service, USDA (United States Department of Agriculture), 2014, “World Agricultural Production, July 11, 2014 World Production, Markets, and Trade Reports”. Retrieved 12 July 2014 from <http://www.fas.usda.gov/data/world-agricultural-production>.
[3] MPOB (Malaysian Palm Oil Board), 2014, “Oil Palm Planted Area”. Retrieved 12 July 2014 from <http://bepi.mpob.gov.my/index.php/statistics/area.html>.
[4] Uemura Y, Omar W, Osman N, Yusup S. Biomass from agricultural sector in Malaysia. J Jpn Inst Energy 2013;92:74–82.
[5] Arias B, Pevida C, Fermoso J, Plaza MG, Rubiera F, Pis JJ. Influence of torrefaction on the grindability and reactivity of woody biomass. Fuel Process Technol 2008;89:169–75.
[6] Prins MJ, Ptasinski KJ, Janssen FJJG. Torrefaction of wood Part 1. Weight loss kinetics. J Anal Appl Pyrolysis 2006;77:28–34.
[7] Prins MJ, Ptasinski KJ, Janssen FJJG. Torrefaction of wood: Part 2. Analysis of products. J Anal Appl Pyrolysis 2006;77:34–40.
[8] Bridgeman TG, Jones JM, Shield I, Williams PT. Torrefaction of reed canary grass, wheat straw and willow to enhance solid fuel qualities and combustion properties. Fuel 2008;87:844–56.
[9] Prins MJ, Ptasinski KJ, Janssen FJJG. More efficient biomass gasification via torrefaction. Energy 2006;31:3458–70.
[10] Uslu A, Faaij APC, Bergman PCA. Pre-treatment technologies, and their effect on international bioenergy supply chain logistics. Techno-economic evaluation of torrefaction, fast pyrolysis and pelletization. Energy 2008;33:1206–23.
[11] Almeida G, Brito JO, Perré P. Alterations in energy properties of eucalyptus wood and bark subjected to torrefaction: the potential of mass loss as a synthetic indicator. Bioresour Technol 2010;101:9778–84.
[12] Phanphanich M, Mani S. Impact of torrefaction on the grindability and fuel characteristics of forest biomass. Bioresour Technol 2011;102:1246–53.
[13] Chen W-H, Kuo P-C. A study on torrefaction of various biomass materials and its impact on lignocellulosic structure simulated by a thermogravimetry. Energy 2010;35:2580–6.
[14] Repellin V, Govin A, Rolland M, Guyonnet R. Modelling anhydrous weight loss of wood chips during torrefaction in a pilot kiln. Biomass Bioenergy 2010;34:602–9.
[15] Deng J, Wang G-J, Kuang J-H, Zhang Y-L, Luo Y-H. Pretreatment of agricultural residues for co-gasification via torrefaction. J Anal Appl Pyrolysis 2009;86:331–7.
[16] Felfli FF, Luengo CA, Suárez JA, Beatón PA. Wood briquette torrefaction. Energy Sustain Dev 2005;9:19–22.
[17] Uemura Y, Omar W, Othman NA, Yusup S, Tsutsui T. Torrefaction of oil palm EFB in the presence of oxygen. Fuel 2013;103:156–60 [available online 19 November 2011].
[18] Rousset P, Macedo L, Commandré J-M, Moreira A. Biomass torrefaction under different oxygen concentrations and its effect on the composition of the solid by-product. J Anal Appl Pyrolysis 2012;96:86–91 [available online 28 March 2012].
[19] Lu K-M, Lee W-J, Chen W-H, Liu S-H, Lin T-C. Torrefaction and low temperature carbonization of oil palm fiber and eucalyptus in nitrogen and air atmospheres. Bioresour Technol 2012;123:98–105 [available online 2 August 2012].
[20] Wang C, Peng J, Xiaotao HL, Bi T, Legros R, Lim CJ. Oxidative torrefaction of biomass residues and densification of torrefied sawdust to pellets. Bioresour Technol 2013;127:318–25 [available online 4 October 2012].
[21] Chen W-H, Lu KM, Lee W-J, Liu S-H, Lin T-C. Non-oxidative and oxidative torrefaction characterization and SEM observations of fibrous and ligneous biomass. Appl Energy 2014;114:104–13 [available online 15 October 2013].
[22] Chen W-H, Lu KM, Liu S-H, Tsai C-M, Lee W-J, Lin T-C. Biomass torrefaction characteristics in inert and oxidative atmospheres at various superficial velocities. Bioresour Technol 2013;146:152–60 [available online 21 Jul 2013].
[23] Eseltine D, Thanapal SS, Annamalai K, Ranjan D. Torrefaction of woody biomass (Juniper and Mesquite) using inert and non-inert gases. Fuel 2013;113:379–88.
[24] Shazleen Saadon, Yoshimitsu Uemura, Nurlidia Mansor, “Torrefaction of Oil Palm Kernel Shell in Oxidizing and Non-oxidizing Environment”, Proceedings for the Annual Postgraduate Student Conference, 2013.
[25] Demirbas A. Mechanism of liquefaction and pyrolysis reactions of biomass. Energy Convers Manage 2000;41:633–46.
[26] Chen W-H, Kuo P-C. Torrefaction and co-torrefaction characterization of hemicellulose, cellulose and lignin as well as torrefaction of some basic constituents. Energy 2011;36:803–11.
[27] Pyle DL, Zaror CA. Heat transfer and kinetics in the low temperature pyrolysis of solids. Chem Eng Sci 1984;39:147–58.
[28] Yang H, Yan R, Chen H, Lee DH, Zheng C. Characteristics of hemicellulose, cellulose and lignin pyrolysis. Fuel 2007;86:1781–8.
[29] Henrich E, Bürkle S, Meza-Renken ZI, Rumpel S. Combustion and gasification kinetics of pyrolysis chars from waste and biomass. J Anal Appl Pyrolysis 1999;49:221–41.
[30] Senneca O. Kinetics of pyrolysis, combustion and gasification of three biomass fuels. Fuel Process Technol 2007;88:87–97.
[31] Kim R-G, Hwang C-W, Jeon C-H. Kinetics of coal char gasification with CO_2: impact of internal/external diffusion at high temperature and elevated pressure. Appl Energy 2014;129:299–307.
[32] Veca E, Adrover A. Isothermal kinetics of char-coal gasification with pure CO_2. Fuel 2014;123:151–7.
[33] Heidari A, Younesi H, Rashidi A, Ghoreyshi A. Adsorptive removal of CO_2 on highly microporous activated carbons prepared from *Eucalyptus camaldulensis* wood: effect of chemical activation. J Taiwan Inst Chem Eng 2014;45:579–88.
[34] Rowell RM, (ed). Handbook of Wood Chemistry and Wood Composites. CRC Press; 2005:p.143.
[35] Uemura Y, Omar WN, Tsutsui T, Yusup S. Torrefaction of oil palm wastes. Fuel 2011;90:2585–91.
[36] Lewin M, Goldstein IS, editors. Wood Structure and Composition. Marcel Dekker. 1991. p.450.
[37] Zhao X, Liu D. Chemical and thermal characteristics of lignins isolated from Siam weed stem by acetic acid and formic acid delignification. Ind Crops Products 2010;32:284–91.